Computational Modeling of Flow inside High Pressure Swirl Injectors By Considering Air-Cavity

M. Rezaeimoghaddam*, M. R. Modarres Razavi, M. B. Ayani, R. Elahi[4]
Ferdowsi University of Mashahad
*m.rezaie.moghaddam@gmail.com

Abstract
In this paper the computational fluid dynamic (CFD) method was used to simulate two-phase flow within high pressure swirl injectors. The two-dimensional axisymmetric swirl Navier-Stokes equations coupled with the Volume-of-Fluid (VOF) method was employed for accounting the formation mechanism of the liquid film inside the swirl chamber and the orifice hole of the high pressure swirl injector. The VOF method was used to identify the liquid-gas interface developing inside the injector. Numerical simulations were carried out under $7MPa$ injection pressure with constant needle injector lift. The time-series analyses were carried out for flow inside injector in the transient state and steady state operation. Numerical results were compared for the steady state operation with experimental and empirical data that available in the literature. Good agreements were obtained for discharge coefficient (C_d) and cone angle (θ) with experimental data.

Keywords: High pressure swirl injectors, Air-Cavity, Volume-of-Fluid, Discharge coefficient, Cone angle

ISME2010-2779

Computational Modeling of Flow inside High Pressure Swirl Injectors By Considering Air-Cavity

M. Rezaeimoghaddam[1], M. R. Modarres Razavi[2], M. B. Ayani[3], R. Elahi[4]

[1]M.Sc. Student, Department of mechanical Engineering, Ferdowsi University of Mashahad; Email: m.rezaie.moghaddam@gmail.com
[2] Professor, Department of mechanical Engineering, Ferdowsi University of Mashahad; Email: m-razavi@ferdowsi.um.ac.ir
[3]Assistant Professor, Department of mechanical Engineering, Ferdowsi University of Mashahad; Email: mbayani@um.ac.ir
[4]M.Sc. Student, Department of mechanical Engineering, Ferdowsi University of Mashahad; Email: r.elahi.msc@gmail.com

Abstract
In this paper the computational fluid dynamic (CFD) method was used to simulate two-phase flow within high pressure swirl injectors. The two-dimensional axisymmetric swirl Navier-Stokes equations coupled with the Volume-of-Fluid (VOF) method was employed for accounting the formation mechanism of the liquid film inside the swirl chamber and the orifice hole of the high pressure swirl injector. The VOF method was used to identify the liquid-gas interface developing inside the injector. Numerical simulations were carried out under $7MPa$ injection pressure with constant needle injector lift. The time-series analyses were carried out for flow inside injector in the transient state and steady state operation. Numerical results were compared for the steady state operation with experimental and empirical data that available in the literature. Good agreements were obtained for discharge coefficient (C_d) and cone angle (θ) with experimental data.

Keywords: High pressure swirl injectors, Air-Cavity, Volume-of-Fluid, Discharge coefficient, Cone angle

Introduction

Tremendous efforts have been carried out in recent years to develop gasoline direct injection (GDI) engines. The GDI engine is one of the most promising internal combustion engines due to achieve lower fuel consumption performance while maintaining low emissions and driving performance. High pressure swirl injectors used in direct gasoline engines are critically important parts of GDI engines because their characteristics have a large effect on engine performance. They are often used in GDI engines because they allow the fine fuel spray at the relatively medium injection pressure. The important geometric parameters in swirl atomizers are tangential slots, a swirl chamber, a needle and a discharge orifice. Figure 1 shows a schematic of a high pressure swirl injector. During the injection process, pressurized liquid is forced to flow through tangential slots into the swirl chamber, rotates in this chamber, and then emerges from the orifice hole in the form of a thin conical sheet due to the creation of an air cavity inside the injector [1].

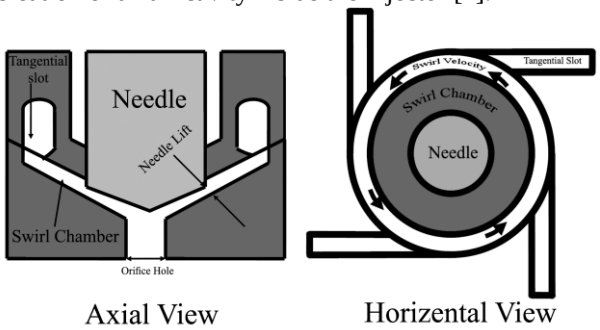

Figure 1: Schematic view of a high pressure swirl injector.

Injector constant defines as a dimensionless parameter was found by Doumas and Laster[2] which is the ratio of inlet area to the product of swirl chamber diameter and exit orifice diameter. The flow characteristics within a pressure-swirl injector are of a highly complex nature due to creation Air-Cavity inside the injector. In the recent years, many studies on swirl injectors have been carried out. Most of the current knowledge is empirical. In 1953 the first studies published by Doumas and Laster [2]. They have developed zero dimensional models where fluids were assumed inviscid. Dumouchel et al [3] studied the two-dimensional viscous flow inside a pressure-swirl injector by numerically solving the streamfunction and vorticity equations. The first three-dimensional computational analysis on internal flow in the high pressure swirl injector was carried out by Ren et al [4]. This approach has been completed and the needle movement inside the injector calculated in transient flows in high pressure swirl injectors by using the FIRE commercial code [5]. The more recent studies as those conducted by Arcoumanis et al [6, 7] take into account both fuel and air flow. Cousin et al [8, 9] investigated zero and one dimensional models in order to find a tool that is not time consuming. The two-dimensional non-swirl computational analysis was carried out by Moon et al [10] with CFD-ACE+ commercial code in order to investigate an optimized injector. Kub et al [11]

simulated the flow inside high pressure swirl injector with viscous model with Star-CD commercial code.

In the current study the two-dimensional Axisymmetric swirl Navier-Stokes numerical model based on VOF technique is employed for accounting the liquid-gas surface interaction inside high pressure swirl injector with cone-type needle. Numerical simulations were computed the volume fraction of each of the fluids in each computational cell throughout the domain. The $k-\varepsilon$ model was used for calculate turbulence effect. Needle lift was assumed to be constant and it equals to 70μ.The inlet total pressure equals the fuel rail pressure fixed at $7\,MPa$ for simulations and the relative outlet pressure equals to zero. In order to compare the numerical results with experimental data two important performance parameters in high pressure swirl injectors are calculated in steady state operation; the discharge coefficient and the cone angle. The discharge coefficient is the ratio of the actual to the maximum theoretical flow rate that is determined from the measured pressure drop across the atomizer.

$$C_d = \frac{\dot{M}_L}{\rho_L A_o \sqrt{2\Delta P/\rho_L}} \tag{1}$$

where $\dot{M}_L$, ρ_L, A_o and ΔP are the mass flow rate of injection liquid, the density of injection liquid, orifice area and the static pressure drop along the injector respectively. The spray cone angle was calculated by:

$$\theta = 2\tan\left(\frac{\overline{W_e}}{\overline{U_e}}\right) \tag{2}$$

where $\overline{W_e}$ and $\overline{U_e}$ are the average swirl and axial velocities at the orifice exit.

The Governing Equations

Numerical simulations of the unsteady two-phase flow field in high pressure swirl injector are governed by the continuity equation (Eq. 3) and Navier-Stokes equations (Eq. 4).

$$\frac{\partial \rho}{\partial t} + \nabla(\rho \vec{u}) = 0 \tag{3}$$

$$\frac{\partial(\rho \vec{u})}{\partial t} + \nabla(\rho \vec{u}\vec{u}) = -\nabla p + \nabla\left[\mu\left(\nabla \vec{u} + \nabla \vec{u}^T\right)\right] + \rho \vec{g} + F_{vol} \tag{4}$$

In spite of the presence of the swirl chamber that creates a Three-Dimensional flow configuration, in this paper due to long time that required for three-dimensional simulation, the two-dimensional axisymmetric swirl model was used for simulate flow through the injector. Due to important role of the swirl velocity in flow inside the injector the tangential momentum equation for two-dimensional swirling flows added to the momentum equations written as follow:

$$\frac{\partial}{\partial t}(\rho w) + \frac{1}{r}\frac{\partial}{\partial x}(r\rho u w) + \frac{1}{r}\frac{\partial}{\partial r}(r\rho v w) = \frac{1}{r}\frac{\partial}{\partial x}\left[r\mu\frac{\partial w}{\partial x}\right] + \frac{1}{r^2}\frac{\partial}{\partial r}\left[r^3\mu\frac{\partial}{\partial r}\left(\frac{w}{r}\right)\right] - \rho\frac{vw}{r} \tag{5}$$

where x is the axial coordinate, r is the radial coordinate, u is the axial velocity, v is the radial velocity, and w is the swirl velocity. The VOF method was used to compute the volume fraction of each of the fluids in each computational cell throughout the domain. In the VOF method, the volume fraction of the first fluid in the cell is denoted as, $\alpha = 0$ for an empty cell; $\alpha = 1$ for a full cell and for partially filled with liquid, α has a value between zero and one. In order to track the position of a free surface between two different phases additional advection equation (Eq. 3) for the additional phase was solved.

$$\frac{\partial \alpha_i}{\partial t} + \vec{u}.\nabla \alpha_i = S \tag{6}$$

Where "S" is the appropriate cavitation mass transfer sink or source term. Due to neglecting the cavitation phenomenon in this study the"S"is considered to be equal to zero. The $k-\varepsilon$ renormalization group (RNG) model was used in order to calculate turbulence effect. The RNG-based $k-\varepsilon$ turbulence model is derived from the instantaneous Navier-Stokes equations, using a mathematical technique. Transport equations for the RNG $k-\varepsilon$ model are as follows:

$$\frac{\partial}{\partial t}(\rho k) + \frac{\partial}{\partial x_i}(\rho k u_i) = \frac{\partial}{\partial x_j}\left(\alpha_k \mu_{eff}\frac{\partial k}{\partial x_j}\right) + G_k + G_b - \rho\varepsilon - Y_M + S_k \tag{5}$$

$$\frac{\partial}{\partial t}(\rho \varepsilon) + \frac{\partial}{\partial x_i}(\rho \varepsilon u_i) = \frac{\partial}{\partial x_j}\left(\alpha_\varepsilon \mu_{eff}\frac{\partial \varepsilon}{\partial x_j}\right) + C_{1\varepsilon}\frac{\varepsilon}{k}(G_k + C_{3\varepsilon}G_b) - C_{2\varepsilon}\rho\frac{\varepsilon^2}{k} - R_\varepsilon + S_\varepsilon \tag{6}$$

where G_k represents the generation of turbulence kinetic energy due to the mean velocity gradients, G_b is the generation of turbulence kinetic energy due to buoyancy. The quantities α_k and α_ε are the inverse effective Prandtl numbers for k and ε, respectively. S_k and S_ε are source terms. The model constants are $C_{1\varepsilon}$ and $C_{2\varepsilon}$ and they were assumed 1.42 and 1.68 respectively [12]. Using the RNG model causes to better handle low-Reynolds-number and near-wall flows .Turbulence, in general, is affected by swirl in the mean flow. The RNG model provides an option to account for the effects of swirl or rotation by modifying the turbulent viscosity appropriately.

Numerical Method

In the numerical simulation the second order upwind scheme was employed to discrete momentum equations and the momentum equations solved implicitly. Also the SIMPLE algorithm substitutes the flux correction equations into the discrete continuity equation to obtain a discrete equation for the pressure correction in the cell. The implicit scheme was employed to discrete VOF equation. Since this equation requires the volume fraction values at the current time step a standard scalar transport equation is solved iteratively for each of the secondary-phase volume fractions at each time step. In this numerical simulation the volume fraction equation was solved once for each time step. This means that the convective flux coefficients appearing in the other transport equations will not be completely updated in each iteration, since the volume fraction fields will not

change from iteration to iteration. In order to track better interface of fuel-gas inside the injector the modified HRIC was used to discrete VOF equation. The modified HRIC scheme is a composite Normalized Variable Diagram (NVD) scheme that consists of a non-linear blend of upwind and downwind differencing. The inlet boundary condition was applied to the top of the swirl chamber of injector. In order to specify the boundary conditions on the inlet the radial and swirl components of the velocity must be calculated from (Eq. 7).

$$W_{inlet} = \frac{Q}{A_p}.\frac{D_s - D_p}{D_s} \text{ and } V_{inlet} = \sqrt{\left(\frac{Q}{A_p}\right)^2 - W_{inlet}^2} \qquad (7)$$

where $W_{inlet}, Q, D_s, D_p, V_{inlet}$ are mean tangential velocity at inlet, static mass flow rate, diameter of swirl chamber, inlet port diameter (inlet port assume to be annular), mean radial velocity at inlet respectively.

Result and Discussion

In the present study the VOF method was used to simulate two-phase flow within high pressure swirl injectors. The mesh independency was studied and around 41,000 quadlateral grid nodes was selected for the solution domain. The N-heptane (C_7H_{16}) was the injected liquid. Calculations were carried out at $7\,MPa$ injection pressure and $300K$ constant temperature. The needles lift were keep constant values (70μ) for the injector. Liquid with uniform axial, radial and swirl velocity is assumed to enter in to the injector from the upper corner of swirl chamber. The magnitude of swirl velocity considered five times greater than radial and axial velocity at the inlet of the swirl chamber.

Brief comparisons between numerical and those of available experiments for characteristic parameters of the injector such as discharge coefficient and spray angle have been shown in table 1 whereas the mass flow rate inside the injector comes in the steady state operation.

Table 1: Comparison of numerical and experimental data predictions

Method	C_d	error	$\theta(\deg)$	error
Current Study	0.115	-4.2%	92.66	+2.9%
Experimental[8]	0.12	-	90.0	-
D. & L. [2]	0.15	+25%	82	-8.9%
1D M. [8]	0.1	-17%	79	-13%

The numerical results show that the differences between the VOF method prediction and experimental data were within -4.2% for discharge coefficient and +2.9% for spray cone angle respectively while the error of Dumas and Laster's method [2] and one-dimensional model [9] estimate at least 4 times greater than VOF method for discharge coefficient and they predict 3 times greater for spray angle than VOF method. The results show a good agreement between VOF simulation and the experimental data. This verification demonstrates VOF model is a reliable method, however other empirical-based algorithm could anticipate fast predictions for these parameters.

After validation, the transient flow inside the injector was simulated and a-time series analyses for transient flow within the injector were carried out. As it can be seen, figure 2 shows the boundary condition for the simulation. Moreover, axisymmetric contours of volume fraction, radial, axial and swirl velocity in time of near beginning (0.044 ms) have been shown in this figure.

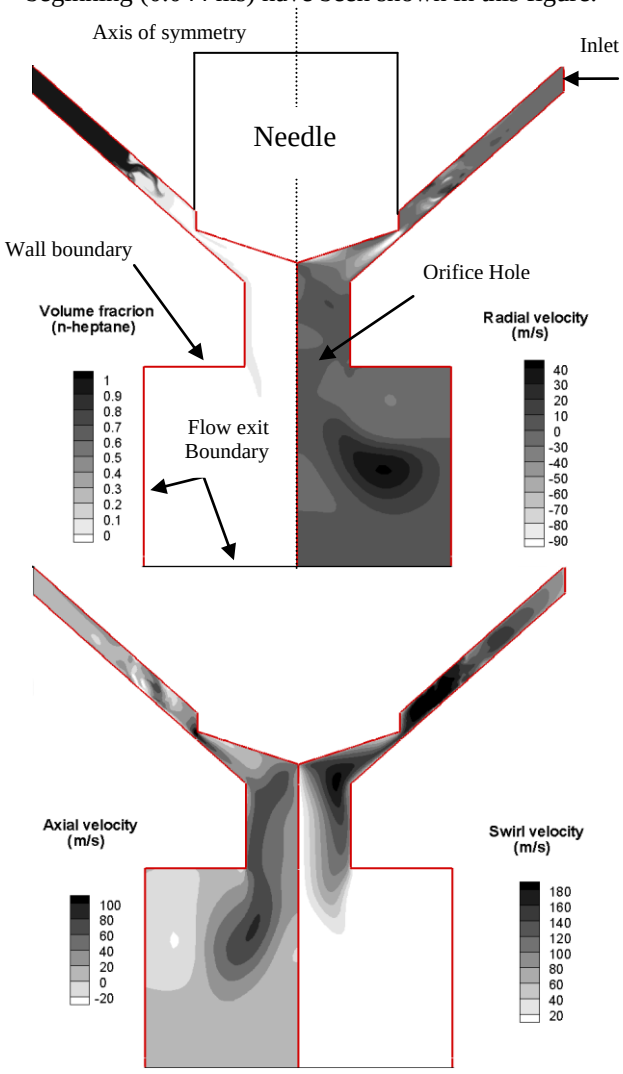

Figure 2: Axisymmetric contours of volume fraction, radial velocity, axial velocity and swirl velocity in 0.044 ms.

When the fuel flow has not been entered into the basic part of the swirl chamber, all velocity characteristics were affected the downstream of domain.

Figures 3, 4 and 5 demonstrate the axisymmetric contours of volume fraction, radial, and swirl velocity in 0.113, 0.196 (transient conditions) and 2.0 ms (steady state operation) respectively. As it can be seen, it is expected that this flow would create a different spray pattern at the early stage of injection relative to that later under steady-state conditions. Also thickness of swirled flow has been changed during these transient conditions. Based on figures 3, 4 and 5, there are three distinguished zones for vortices; (a) inlet swirl slot before needle with several minor vorticity in liquid phase, (b) diverging zone after minimum passage area which is placed exactly below of needle surface with vortices in both phases and (c) two major vortices

besides of outflow spray film in downward gas flow which are circulate in opposite spin of each other. While, three-dimensional flow characteristics create a two-phase complex flow around the domain, the vortices in both liquid and gas affect downstream parameters such as spray angle and general downward velocity profile.

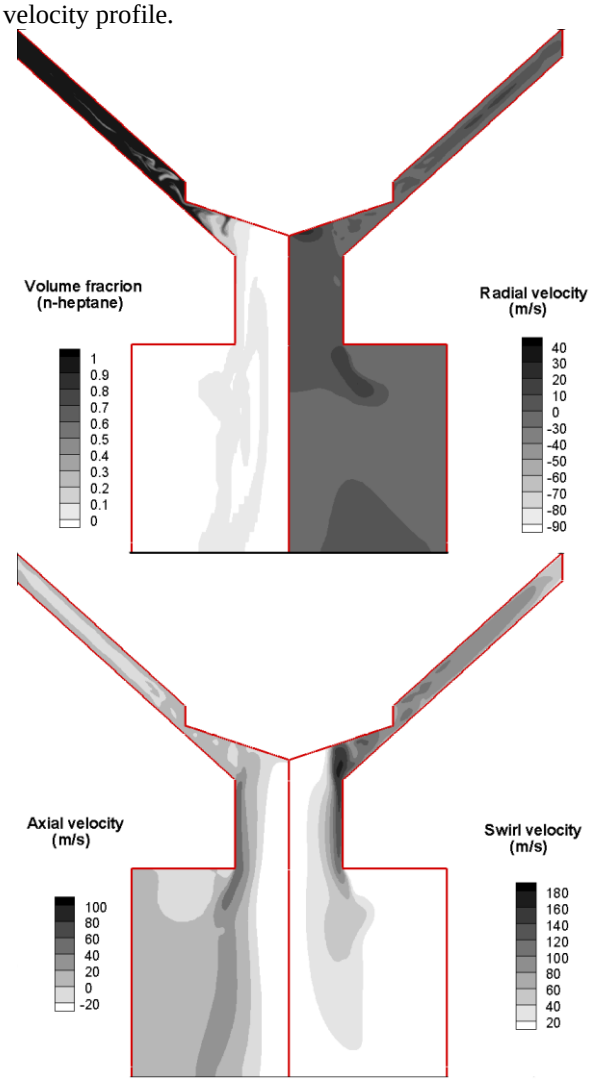

Figure 3: Axisymmetric contours of volume fraction, radial velocity, axial velocity and swirl velocity in 0.131 ms

Velocity vectors and pressure domain in different time steps are shown in figure 6. Based on the injector geometry, several three-dimensional vortices have been occurred into flow before needle passage. Also, low pressure zone starts to grow in upper side of diverging passage and the velocity profile shaped with its maximum nearby the swirl chamber surface. A considerable vorticity has been expand in low pressure area and this phenomenon assist the flow to have wider spray angle and regulate the mass flow rate in steady state condition. The pressure drops gradually within the swirl chamber and becomes equal to the back pressure in the area of discharge hole by the liquid film.

Calculated axial velocities at the discharge hole in different times are shown in figure 7. Maximum point of profile has been moved through the wall of orifice hole during the time. With comparing the axial velocity profiles in the figure 7 and liquid region in figures 2 to 5, it is clearly understood that the velocity profile shows the liquid interface. On the whole, the liquid-gas interface placed commonly in region of the velocity profile whereas the magnitude of velocity changes sharply. Also when the liquid passed through the discharge hole, the gas velocity has an opposite direction based on the third vorticity region in the domain.

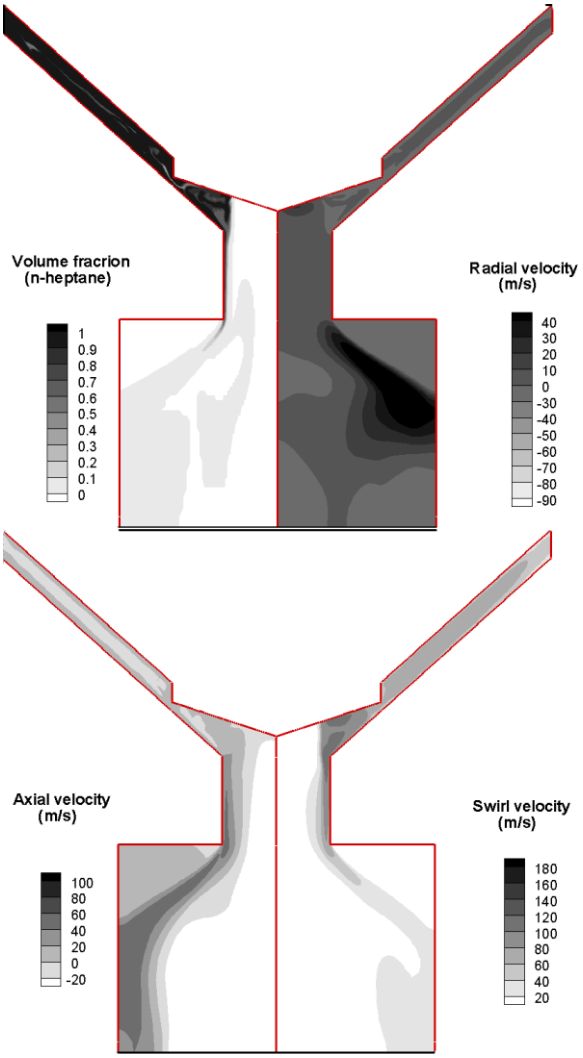

Figure 4: Axisymmetric contours of volume fraction, radial velocity, axial velocity and swirl velocity in 0.196 ms

Calculated radial velocity profile at the discharge hole in different times is also illustrated in the figure 8. However, the maximum magnitude of the radial velocity is about three to five times less than the maximum magnitude of the axial velocity at the same time. Opposite velocity direction between gas and liquid is also observed considering to create a complex three dimensional flow around the chamber.

In addition, figure 9 is shown the calculated swirl velocity at the discharge hole in different times. As it can be seen the swirl velocity magnitude has values in order of axial velocity, also the flow regime in this direction is very similar to other directions.

Considering a detailed investigation into transient process the variation of calculated mass flow rate with time at the inlet of swirl chamber is shown in figure 10. Initial high flow rate of 0.04 kg/s has been reduced

based on effect of swirl, vorticity and pressure losses into 0.01 kg/s whereas steady state condition obtained. During the transient process mass flow rate fluctuation has been occurred based on the first downstream lower pressure and increasing the pressure during the time. Because of subsonic flow filled in the injector, downstream characteristic flow parameters could be changed the inlet parameters such as mass flow rate.

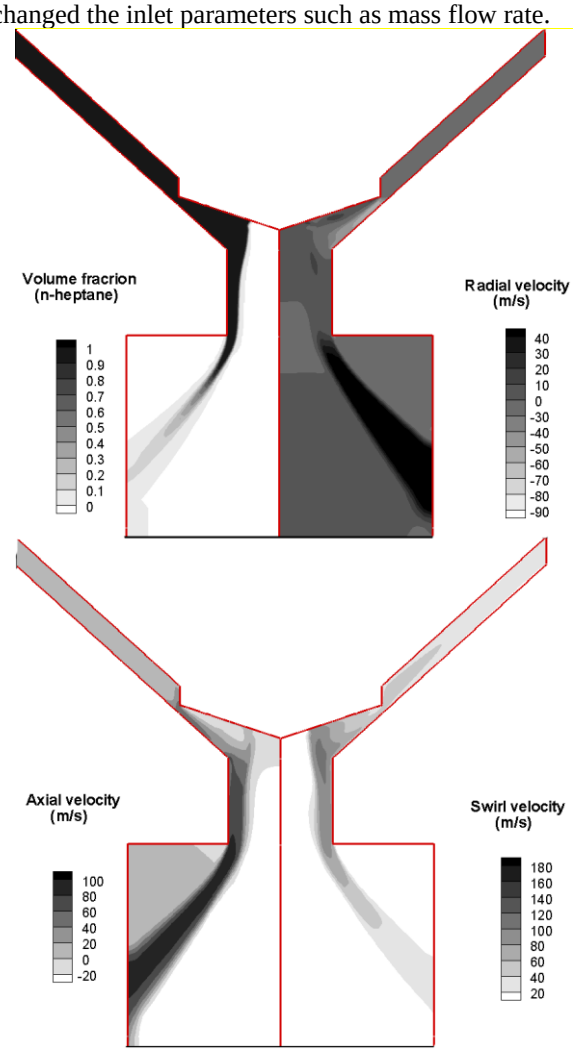

Figure 5: Axisymmetric contours of volume fraction, radial velocity, axial velocity and swirl velocity in 2.0 ms

Conclusion

The two-phase flow inside high pressure swirl injectors was simulated. The VOF method was employed to track the surface between the fluid and air through the injector consisting of fuel and air that form the Air-Cavity. The time series analyses were carried out to investigate volume fraction of fuel, axial, swirl and radial velocity the injector. Calculations showed after 2ms the mass flow rate fluctuation was dumped and the mass flow rate keeps constant value (steady state operation). Numerical results have shown that the critical properties of the injector design such as cone angle and discharge coefficient can be calculated with good accuracy compared with the other empirical formulas. The VOF method predicts accurate the air-cavity inside the injector and it leads to obtain a more accurate estimate size of the spray droplet that expels from the orifice hole of the injector.

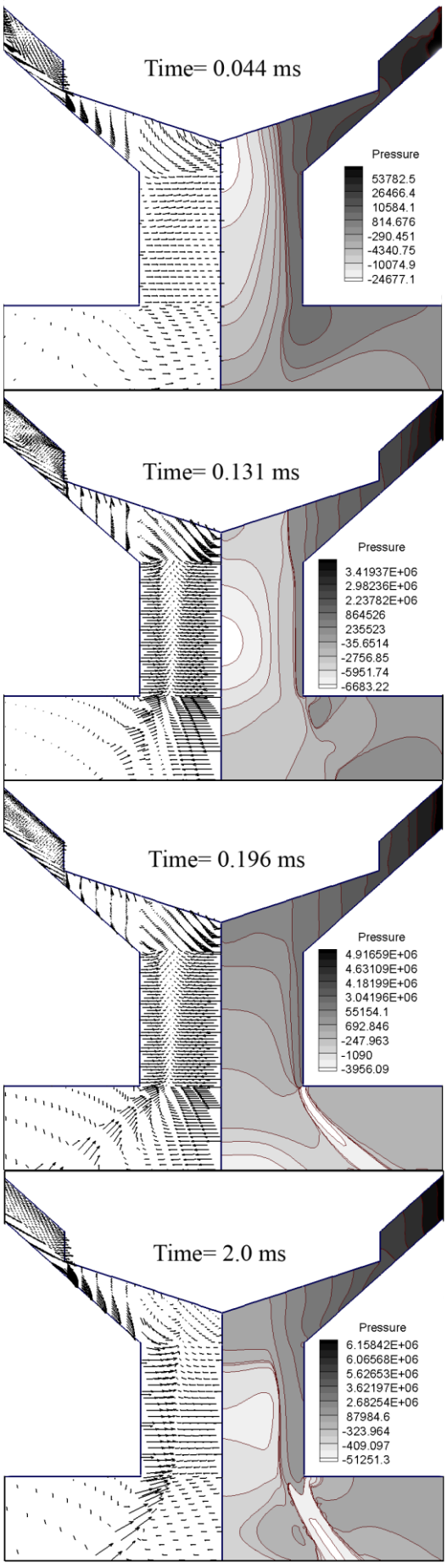

Figure 6: Velocity vectors and pressure domain in different time steps.

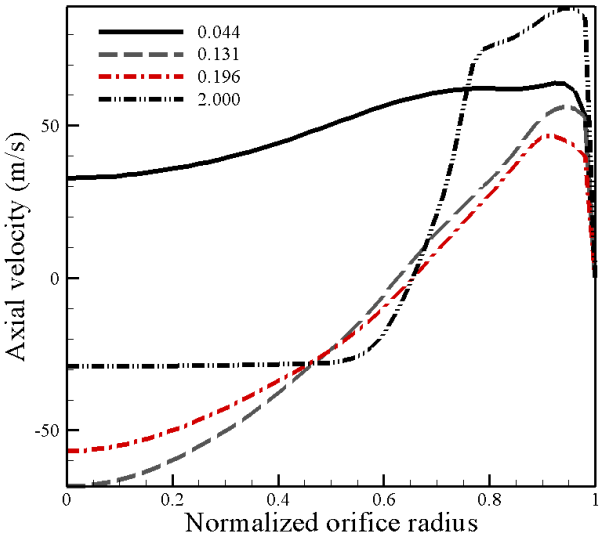

Figure 7: Calculated axial velocity at the discharge hole in different times.

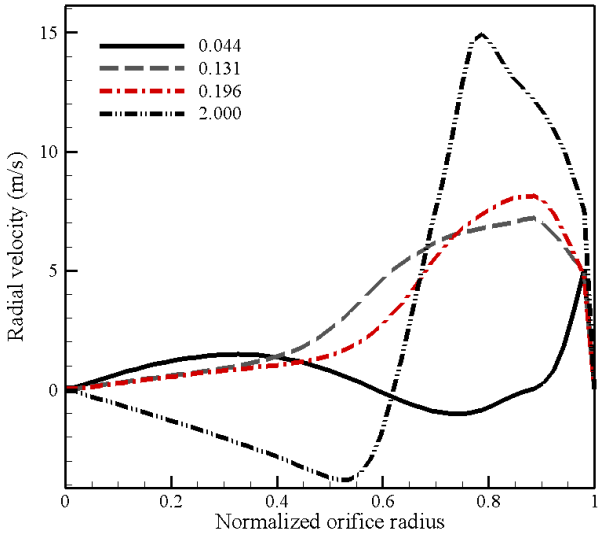

Figure 8: Calculated radial velocity at the discharge hole in different times

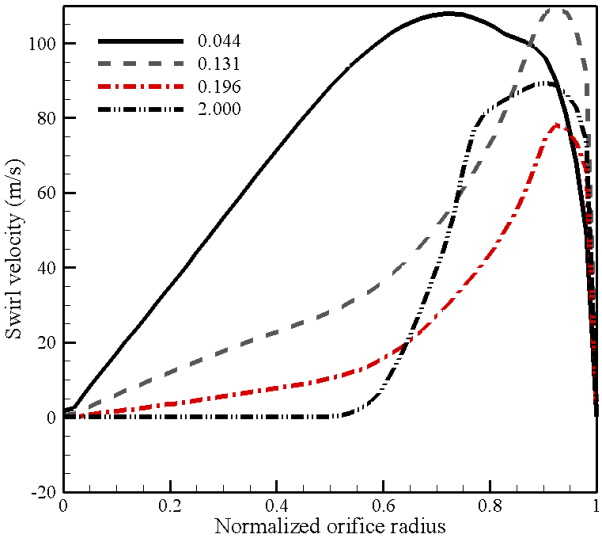

Figure 9: Calculated swirl velocity at the discharge hole in different times

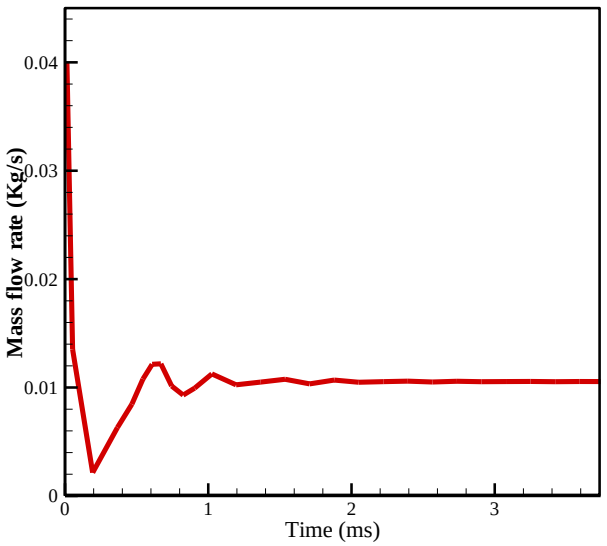

Figure 10: Variation of calculated mass flow rate with time at the inlet of swirl chamber

References

[1] Lefebvre, A. H., 1989, Atomization and Spray, Hemisphere Publishing Co.

[2] M. Doumas, R. Laster,1953,"Liquid-Film Properties for Centrifugal Spray Nozzles" *Chemical Engineering Progress*, pp.518-526.

[3] C. Dumouchel, M. I. G. Bloor, N. Dombrowski, D. B. Ingham, and M. Ledoux, 1993,"Viscous Flow in a Swirl Atomizer" *Chemical Engineering Science*, vol. 48, no. 1, pp. 81- 87.

[4] W. M. Ren, J. Shen, and J. G. Nally, 1997, "Geometric Effects Flow Characteristics of Gasoline High Pressure Swirl Injector". *SAE Technical Paper No. 971641*, pp.1790-1797.

[5] J. Cousin, W. M. Ren, S. Nally,1998,"Transient Flows in High Pressure Swirl Injectors" *SAE Technical Paper No. 980499.*

[6] C. Arcoumanis, M. Gavaises,1999, "Modeling of Pressure Swirl Atomizers for GDI Engines", *SAE Technical paper No 1999-01- 0500*, pp. 516-532.

[7] C. Arcoumanis, M. Gavaises, 2000, "Pressure Swirl Atomizers for DISI Engines: Further Modeling and Experiments", *SAE Technical paper No 2000-01-1044*,pp.

[8] J. Cousin, H. J. Nuglisch, 2001,"Modeling of Internal Flow in High Pressure Swirl Injectors" *SAE Technical paper No 2001-01- 0963*.

[9] J. Galpin, J. Cousin, G. Corbinelli, S. Sivieri, 2005, "A One Dimensional Model for Designing Pressure Swirl Atomizers" *SAE Technical paper No 2005-01-2101*.

[10] S. Y. Moon, S. H. Bae, C. W. Lee, 2001," Optimized Design of A New Gasoline Direct Swirl Injector" *Journal of Numerical Heat Transfer Part A*,pp.157-167

[11] M. Kubo, A. Sakakida, A. Liyama, 2001," Technique for Analyzing Swirl Injectors of Direct-Injection Gasoline Engines" *SAE Technical paper No 2001-01-0964.*

[12] S. H. Lam, 1992, "On The RNG Theory of Turbulence" *Journal of Physics of Fluid*, A,4,pp.1007-1017.